Interlayer electronic superfluid in an external magnetic field in graphene double layers

Andreas Sinner [*]
Institute of Physics, University of Opole, 45-052 Opole, Poland

(Received 31 March 2023; revised 16 June 2023; accepted 22 June 2023; published 5 July 2023)

We investigate the formation mechanism of the recently proposed interlayer electronic superfluid state due to repulsive interaction in graphene double layers. Using the renormalization group argumentation we show how the emergence of a particular interlayer staggered order parameter wins the competition between several possible pairing mechanisms. We determine the effective action for the fluctuations of the order parameter and study its behavior in strong background magnetic fields. The filling factors obtained from the constraint conditions put on this action are in qualitative agreement with the previously experimentally observed results.

DOI: 10.1103/PhysRevB.108.024502

I. INTRODUCTION

Even after having been studied for several decades [1–3] the superfluidity of paired objects in layered electronic and electron-hole systems keeps attracting substantial attention, both experimentally and theoretically [4,5]. In particular, nearly two decades of graphene-based bilayer studies [6–8] have revealed partially unexpected physics, e.g., the proposed room temperature superconductivity [9] or flat-band superconductivity in twisted graphene bilayers, which was recently found in a series of spectacular experiments [10,11] based on earlier theoretical studies [12,13]. Moreover, these systems continue to represent the playground for proposing new physical effects and their experimental detection. For instance, the condensation of paired objects in electronic multilayers due to strong repulsive interaction has long been proposed [14]. In our recent work we have considered the possibility for the pairing formation due to repulsive interactions between electrons in the layered systems consisting of either two layers hosting Dirac electron gas [15] or heterostructures with Dirac and conventional electron gases [16] in each layer. For the pairing mechanism of two Dirac electron species described in Ref. [15] a duality between electron-electron and electron-hole systems has been stressed, which suggest an equivalence with the exciton condensation of electron-hole pairs. Moreover, an anomalous Josephson effect for this phase has been proposed in Ref. [17].

The phenomenology of the pairing transition between two Dirac fermion gases due to mutual repulsion suggests emergence of the staggered order parameter, which anticommutes with the interaction-free Hamiltonian and therefore has a stable mean-field solution. It is difficult to anticipate the emergence of such an order parameter from the most general interaction between the electron densities from different layers. It needs to be shown how this pairing order parameter emerges from the simple Hubbard-like interaction and prevails in the competition with the other possible pairing channels. In this paper we resolve this question using the Fierz-like transformations of the interaction and the renormalization group. The former allows for the representation of the interlayer Hubbard-like interaction in terms of different interlayer pairing order parameters, and the renormalization group (RG) flow sheds light on the competition between them. The RG flow of the relevant coupling parameter reveals a singularity, called the Landau pole. The scale at which this singularity occurs is in a qualitative agreement with the onset of the pairing order parameter which follows from the corresponding mean-field equation.

After completing this preparatory work, we turn our attention to the studies of the behavior of that state in the strong magnetic field. Recent experiments Refs. [18–20] reported a measurement of interlayer fractional quantum Hall states, which appear in vertically stacked double layers perfectly aligned in an AA stacking. The interpretation of these experiments suggests that upon bringing two two-dimensional (2D) conducting layers to proximity, a new set of correlated states can emerge due to interactions between electrons in both layers. The experimental setup realizes an electric separation of both layers by a thing isolating film which suppresses the interlayer electron hopping. This phenomenological picture is remarkably reminiscent to the interlayer electron-electron-pairing mechanism suggested by us in Ref. [15]. In the presence of strong magnetic field one observes the emergence of a topological quantum Hall liquid state due to charged interlayer Bose-Einstein condensate. The analysis of experiments of Refs. [18–20] in terms of the composite fermion theory [21] assumes the phenomenon of the flux attachment to the charged particle. Microscopically, the flux attachment is captured by the introduction of an internal Chern-Simons gauge field, which couples to the charged particle. Since the gauge field couples to the matter minimally, i.e., via covariant derivative, one needs to determine the low-energetic dynamics of the order parameter. This happens to be given in terms of a Lorenz-invariant effective action, rather than the Galilean-invariant action similar to the Zhang, Hannson, and Kivelson (ZHK) model [22,23]. From this action we extract

[*]andreas.sinner@uni.opole.pl

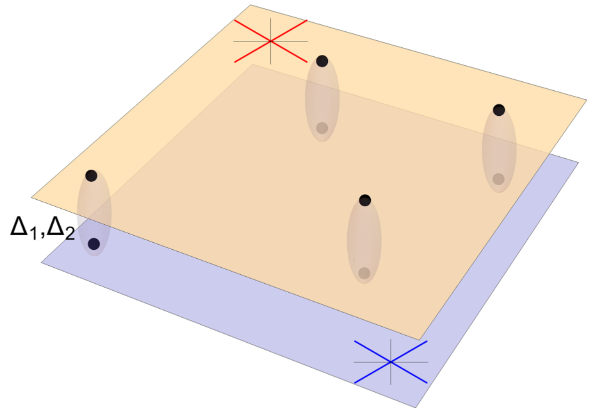

FIG. 1. The schematic representation of the studied system: The Dirac particles dwelling in the individual layers form interlayer paired states shown by the gray clouds.

the expression for the filling factors and argue that they are in qualitative agreement with the observed sequences of the fractional quantum Hall sates. The interaction and correlation physics in different realizations of graphene double-layers and bilayers have been intensively studied for almost two decades. We especially emphasize the importance of Refs. [24–30] for our work.

Structurally the paper is organized as follows: In Sec. II we introduce the model and discuss the heuristic approach to the mean-field equations for the order parameter of the paired state. In Sec. III we discuss the renormalization group equations which describe the competition between different channels, which appear in the interaction after its reordering using the Fierz identities. In Sec. IV we decouple the effective interaction using a suitable Hubbard-Stratonovich transformation and determine the effective action, which governs the dynamics of the fluctuations of the order parameter. By attaching the magnetic field to the energetically lower branch of the fluctuations we arrive at the above-mentioned effective model in Sec. V. We discuss the consequences from this fact for the Chern-Simons electrodynamics and extract the filling factor for the corresponding fractional quantum Hall states. The lengthy computational passages are placed into the Appendices.

II. THE MODEL

We adopt the model formulated in Ref. [15]. It describes in a simplified form the pairing of electrons which reside in two layers of graphene. For both graphene layers we assume a strict AA orientation, which implies an exact matching of both honeycomb lattices and correspondingly interlayer hopping processes between the same sublattices. Nonetheless, the AA stake is perfectly realizable in an experimental setup [31]. Our first intention is to perform the renormalization group analysis, which is more convenient to do in the functional integral formalism. We show the considered system in Fig. 1. For a bipartite honeycomb lattice at half-filling we introduce a sublattice representation, at which each lattice site at the coordinates $\mathbf{r}$ is populated by two-component fermions. Then the hopping Hamiltonians H_s ($s = \uparrow, \downarrow$) read in terms of fermionic creation (annihilation) operators $\hat{c}^\dagger_{s;\mathbf{r}}$ ($\hat{c}_{s;\mathbf{r}}$)

$$H_s = \sum_{j=1}^{2} \sum_{\mathbf{r},\mathbf{r}'} h_{j;\mathbf{r}\mathbf{r}'} \hat{c}^\dagger_{s;\mathbf{r}} \cdot \sigma_j \hat{c}_{s;\mathbf{r}'}, \tag{1}$$

where $\sigma_{j=1,2}$ are Pauli matrices. The fermionic annihilation operators are written as column vectors $\hat{c}_{s;\mathbf{r}} = (c_{s;\mathbf{r}},\ d_{s;\mathbf{r}})^{\mathrm{T}}$, whose upper (lower) component refers to sublattice A (B). The interaction term reads

$$H_I = \frac{g}{2} \sum_{\mathbf{r}} n_{\uparrow\mathbf{r}} n_{\downarrow\mathbf{r}}, \quad n_{s\mathbf{r}} = c^\dagger_{s\mathbf{r}} c_{s\mathbf{r}} + d^\dagger_{s\mathbf{r}} d_{s\mathbf{r}}. \tag{2}$$

Recent experimental breakthroughs in manipulating graphene bilayers Ref. [10,11] give strong support to the thesis, that all main effects of the graphene bilayer physics can be very well understood within the simplified approach taking a single Dirac fermion into account, in which the effects of internode scattering in each layer or between nodes with different chirality in opposite layers of the bilayer can be ignored. This thesis does also find strong theoretical support in Refs. [12,13]. Thus, in low-energy approximation we retain only one Dirac point in Eq. (1) in the kinetic energy part and also neglect the internodal contribution in the interaction term. This is not dictated by an anticipated technical effort, but rather by our wish to shape the analysis in a most transparent way. We comment on several places in the text on the analogies to the two-cone model. With these simplifications, the bare action of the system reads

$$\mathcal{S} = \sum_{s=\uparrow,\downarrow} \psi^\dagger_s \cdot [\partial_\tau + h]\psi_s + \frac{g}{2}(\psi^\dagger_\uparrow \psi_\uparrow)(\psi^\dagger_\downarrow \psi_\downarrow), \tag{3}$$

where $h = i\nabla \cdot \sigma$ and $\psi_{\uparrow,\downarrow}$ are the Grassmann fields, which appear in the action in place of operators in the coherent states basis, cf. Appendix A. The interaction is local and instantaneous, and the summation over the spinor indices and integration over the position space and imaginary time is understood. The introduction of different correlation channels in the interlayer space, which ultimately give rise to different pairing order parameters, is achieved with the help of fermionic transformations similar in the spirit to the so-called Fierz identities [32]

$$\mathcal{S}_g = \frac{g}{2}(\psi^\dagger_\uparrow \psi_\uparrow)(\psi^\dagger_\downarrow \psi_\downarrow) = -\frac{g}{4}(\psi^\dagger_\uparrow \sigma_\mu \psi_\downarrow)(\psi^\dagger_\downarrow \sigma_\mu \psi_\uparrow), \tag{4}$$

where it is summed over $\mu = 0, 1, 2, 3$ and σ_μ are the Pauli matrices and the 2D unity matrix (σ_0) in usual representation. The details of the transformation are summarized in Appendix A. This factorization can be also generalized to the case of nonlocal extended interactions, cf. Ref. [33]. Factorizations of that kind are by no means unique to the single-cone model. A model which takes both cones can be factorized in the same way, but using instead 16 Dirac matrices $\Sigma_{\mu\nu} = \sigma_\mu \otimes \sigma_\nu$. For Ψ_s being a four-component bispinor, the Hubbard-like interaction would transform as

$$(\Psi^\dagger_\uparrow \Psi_\uparrow)(\Psi^\dagger_\downarrow \Psi_\downarrow) = -\tfrac{1}{4}(\Psi^\dagger_\uparrow \Sigma_{\mu\nu} \Psi_\downarrow)(\Psi^\dagger_\downarrow \Sigma_{\mu\nu} \Psi_\uparrow), \tag{5}$$

which can be checked with some effort, cf. Appendix A 2. The manipulations with such interactions become considerably more cumbersome with not much additional physical gains when compared to the simple one-cone model. The way particular interaction channels are introduced here differs from the considerations of Refs. [24,25]. These works study the superconductivity in graphene with considerable doping, which lifts the Fermi surface up to the saddle points in the spectrum at approximately 3 eV. The highly populated states residing at these points give rise to van Hove singularities in the density of states and interact with each other over a plethora of repulsive interactions, which are deduced by means of "fermionology" or "g-ology" of possible scattering processes. This approach is very different in its nature to the one pursued in the present paper. Here different channels are not deduced but appear as a consequence of a suitable representation of the original simple interaction.

In Ref. [15] we made the assumption that among four complex order parameters Δ_μ recognizable from the interaction Eq. (4) and given by the self-consistent equations

$$\Delta_\mu = -\frac{g}{4}\langle\psi_s^\dagger\sigma_\mu\psi_{s'}\rangle, \tag{6}$$

the one with $\mu = 3$ is the most dominant. The corresponding equation reads

$$\Delta = \frac{g}{4}\mathrm{tr}\{\sigma_3\langle\psi_{s'}\psi_s^\dagger\rangle\} \tag{7}$$

and describes the staggered order parameter with opposite signs on both sublattices. The emergent phase describes the pairing between the electrons from the opposite layers. Therefore the correlator $\langle\psi_{s'}\psi_s^\dagger\rangle$ represents the off-diagonal term of the local Green's function

$$G(X,X) = \begin{pmatrix} \partial_\tau + h & \Delta\sigma_3 \\ \Delta^*\sigma_3 & \partial_\tau + h \end{pmatrix}^{-1}_{X,X}. \tag{8}$$

Inverting the matrix and dropping the rotationally noninvariant terms we get

$$G(X,X) = \int^\Lambda \frac{d^2q}{(2\pi)^2}\int\frac{dq_0}{2\pi}\,\frac{1}{q_0^2+q^2+|\Delta|^2}\begin{pmatrix} 0 & \Delta\sigma_3 \\ \Delta^*\sigma_3 & 0 \end{pmatrix}. \tag{9}$$

Inserting the Greens function into the Eq. (7) yields the usual condition for the nontrivial phase

$$1 = \frac{g}{2}\int^\Lambda \frac{d^2q}{(2\pi)^2}\int\frac{dq_0}{2\pi}\,\frac{1}{q_0^2+q^2+|\Delta|^2}. \tag{10}$$

The solutions for this type of equations are well known and can be found elsewhere, e.g., Ref. [33]. For our purposes it is important to recognize that this equation is intrinsically related to the notion of the Landau pole, i.e., to the singularity in the renormalization group flow of the coupling parameter g. The analog of the order parameter Eq. (7) for the model with two cones in each layer and interaction Eq. (5) is explained in Appendix A 3.

III. RENORMALIZATION GROUP ANALYSIS

The main point for the criticism of the analysis presented in the previous section is, that it assumes *a priori*, that σ_3 channel somehow wins in the competition against the others. Our task now is to give a firm support to this claim by means of the renormalization group (RG). The main idea is to let each Pauli channel evolve under RG transform intependently. For this we modify the interaction term

$$\mathcal{S}_g = -\frac{g_\mu}{4}(\psi_\uparrow^\dagger\sigma_\mu\psi_\downarrow)(\psi_\downarrow^\dagger\sigma_\mu\psi_\uparrow), \tag{11}$$

where the four coupling parameter have the same initial value only at the start of the RG flow $g_\mu(0) = g$. Splitting the Grassmann fields in fast and slow components $\psi_s \to \psi_{s,<} + \psi_{s,>}$, the action Eq. (3) separates into the terms containing only slow/fast fields $\mathcal{S}^<, \mathcal{S}^>$. Correspondingly, the interaction term Eq. (11) splits into the term topologically identical to Eq. (11) comprising only of slow fields and mixed terms

$$\mathcal{S}_g \to \mathcal{S}_g^< + \delta\mathcal{S}_g^{<,>}. \tag{12}$$

In the latter we integrate out fast terms perturbatively

$$e^{-\delta\mathcal{S}^<} \approx \langle e^{-\delta\mathcal{S}^{<,>}}\rangle_> \approx \left\langle 1 - \delta\mathcal{S}^{<,>} + \tfrac{1}{2}\delta\mathcal{S}^{<,>}\delta\mathcal{S}^{<,>}\right\rangle_>. \tag{13}$$

Since the electronic propagators have no interlayer terms, this must be taken into account in functional integrations. In particular only fields from the same layer can be contracted. The detailed discussion of the diagrams is presented in Appendix B 1. Here we only give the final important results. The only allowed diagrams are shown in Fig. 2. The leading order self-energy correction is zero by angular integration. The process which renormalizes the bare interaction vertex is given by the second diagram ("bubble"). It reads

$$\tilde{g}_\mu = -\frac{g_\mu^2}{16}\mathrm{Tr}\int\frac{d^3Q}{(2\pi)^3}\,G(Q)\sigma_\mu G(Q)\sigma_\mu. \tag{14}$$

The correction turns out to be diagonal in the Pauli channel indices μ due to the combined action of the trace over Pauli matrices and angular integration. We evaluate Eq. (14) for each combination of channel indices in Appendix B 2. Here we only present the final result of these calculations:

$$\partial_\ell g_0 = 0, \quad \partial_\ell g_{1,2} = \frac{g_{1,2}^2}{32}\frac{\Lambda_0}{2\pi}, \quad \partial_\ell g_3 = \frac{g_3^2}{16}\frac{\Lambda_0}{2\pi}. \tag{15}$$

The equation for g_0 suggests its absolute marginality to one-loop order. The analysis of two further equations becomes more transparent after rescaling the interaction strength as $g_i \to 32\pi g_i/\Lambda_0$. In case of g_3 this gives

$$\partial_\ell g_3 = g_3^2, \tag{16}$$

which has the solution

$$g_3(\ell) = \frac{g}{1-g\ell}, \tag{17}$$

with the initial condition $g_3(0) = g$. At $\ell_* = g^{-1}$ the solution has a singularity, known as the Landau pole. Analogous evaluation of the RG equation for $g_{1,2}$ yields

$$g_{1,2}(\ell) = \frac{2g}{2-g\ell}, \tag{18}$$

which also has a Landau pole, which however lies at much higher energy and is therefore subordinate to the singularity of g_3. Restoring the original scaling of the interaction strength, the Landau pole position for g_3 is at

$$1 = \frac{g}{16}\frac{\Lambda_0}{2\pi}\ell_* = \frac{g}{16}\frac{\Lambda_0}{2\pi}\log\frac{\Lambda_0}{\Lambda_*}, \tag{19}$$

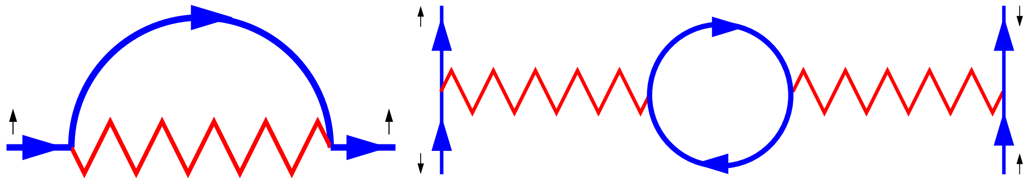

FIG. 2. Allowed first- and second-order perturbative processes.

from where the relevant energy scale can be extracted $\Lambda_* = \Lambda_0 \exp[-32\pi/g\Lambda_0]$. Up to an irrelevant constant factor, this result also follows from the mean-field condition Eq. (9) for $\Delta = 0$ and momentum integration being carried out over the thin shell. The Landau pole is therefore imprinted into the mean-field equation. Close to the Landau pole the σ_3 channel becomes dominant and we can surely ignore all other channels. The singularity in turn manifests the breaking down of the perturbative approach and justifies changing to the mean-field framework. On the physical side, to avoid the Landau pole singularity, the system reorganizes by forming the condensate of the coupled electrons from opposite layers. Phenomenologically, this transition has been analyzed in Ref. [15]. An instability similar in spirit has been reported earlier in Ref. [30].

IV. BEYOND THE MEAN-FIELD ANALYSIS: THE FLUCTUATIONS OF THE ORDER PARAMETER

The analysis of the fluctuations is almost exclusively done in the functional integral formalism. At energy scale close to the Landau pole we replace the initial action Eq. (3) by

$$\mathcal{S} = \sum_{s=\uparrow,\downarrow} \psi_s^\dagger \cdot [\partial_\tau + h]\psi_s - \frac{g}{4}(\psi_\uparrow^\dagger \sigma_3 \psi_\downarrow)(\psi_\downarrow^\dagger \sigma_3 \psi_\uparrow), \quad (20)$$

where we now use simply g in place of original g_3. The interaction term is decoupled by means of the suitable Hubbard-Stratonovich transformation

$$\begin{aligned} &-\frac{g}{4}(\psi_\uparrow^\dagger \sigma_3 \psi_\downarrow)(\psi_\downarrow^\dagger \sigma_3 \psi_\uparrow) \\ &\quad\to \frac{1}{2g}\mathcal{Q}^*\mathcal{Q} + \frac{1}{2\sqrt{2}}(\psi_\uparrow^\dagger \mathcal{Q}^* \sigma_3 \psi_\downarrow) \\ &\qquad + \frac{1}{2\sqrt{2}}(\psi_\downarrow^\dagger \mathcal{Q} \sigma_3 \psi_\uparrow). \end{aligned} \quad (21)$$

The constant prefactors can be removed by rescaling the Hubbard-Stratonovich fields as $\mathcal{Q} \to 2\sqrt{2}\mathcal{Q}$, which then leads to the decoupled action

$$\mathcal{S}[\mathcal{Q}, \Psi] = \frac{4}{g}\vec{\mathcal{Q}} \cdot \vec{\mathcal{Q}} + \Psi^\dagger \cdot \big[G_0^{-1} + \vec{\mathcal{Q}} \cdot \hat{\Sigma}\big]\Psi. \quad (22)$$

Here we decomposed the complex Hubbard-Stratonovich fields into their real and imaginary parts $\mathcal{Q}^\# \to \mathcal{Q}_1 \pm i\mathcal{Q}_2$ and introduced $\vec{\mathcal{Q}} \cdot \hat{\Sigma} = \mathcal{Q}_1\Sigma_{13} + \mathcal{Q}_2\Sigma_{23}$, where the vector $\hat{\Sigma} = \{\Sigma_{13}, \Sigma_{23}\}$ and the inverse propagator of free Dirac particles $G_0^{-1} = \partial_\tau \Sigma_{00} + i\nabla_1\Sigma_{01} + i\nabla_2\Sigma_{02}$ using some of the 16 matrices $\Sigma_{ij} = \sigma_i \otimes \sigma_j$, $i, j = 0, 1, 2, 3$ mentioned before. With exception of the unity matrix Σ_{00} all matrices appearing in the action mutually anticommute, which makes the inversion of the matrix particularly simple. Integrating out the fermions leads to the nonlinear action

$$\mathcal{S}[\mathcal{Q}] = \frac{4}{g}\vec{\mathcal{Q}} \cdot \vec{\mathcal{Q}} - \operatorname{tr}\log\big[G_0^{-1} + \vec{\mathcal{Q}} \cdot \hat{\Sigma}\big], \quad (23)$$

which is then expanded in powers of $\vec{\mathcal{Q}} \cdot \hat{\Sigma}$, that is in inverse powers of the superconducting gap parameter Δ. The details of the evaluation are put into the Appendix C. The nontrivial saddle point of this action yields the saddle-point equations identical with Eq. (9). Expansion in fluctuations to the second order reveals the presence of a gapless mode already reported in Ref. [15]. However, its spectrum acquires a mass through the coupling to the other mode to cubic order. The unbinding of both modes at a global minimum to the fourth-order expansion term reveals a surprisingly simple structure of the low-energetic effective action

$$\mathcal{S}[\varphi] = \frac{2}{\pi}\Delta^3\bigg[\frac{1}{2}\varphi \cdot \big[-\xi^2\partial_\mu^2\big]\varphi - \frac{1}{2}\varphi^2 + \frac{1}{4}\varphi^4\bigg]. \quad (24)$$

The real dimensionless (i.e., rescaled in units of the mean-field gap) fields φ represent the fluctuations of the field $\mathcal{Q}_2$ above the mean-field gap Δ, cf. Appendix C. They have only Ising Z_2 symmetry. $\xi = (2\Delta)^{-1}$ is the correlation length. The corresponding stationary expression has a form typical for the Ginzburg-Landau free-energy functionals. Without an external magnetic field, the action of this type shows instability towards the formations of the solitons [34]. The formation of the soliton follows from the solution of the instanton equation

$$-\frac{\delta}{\delta\varphi}\mathcal{S}[\varphi] = 0 = 2\frac{\Delta^3}{\pi}\big[\xi^2\partial_\mu^2\varphi + \varphi - \varphi^3\big], \quad (25)$$

for which the existence of the time-independent solutions is forbidden by the Derrick's theorem, though, cf. Ref. [31] in [34]. If however the system is subject to an external magnetic field, then this action describes the formation of the vortices (with a $\mathcal{Z}_2$ symmetry in this particular case). In $d = 2$, however, vortices relate to the the fractional quantum Hall effect [35]. Let us now switch on the magnetic field in the system with the condensate. Because the condensate is built of charged particles, it fills the presence of the magnetic field and sticks to it.

V. FRACTIONAL FILLING FACTORS IN QUANTUM HALL REGIME

Without magnetic field, the gap fluctuation field φ is shown to be real, i.e., it cannot have any phase. With the magnetic field the situation must change. In this case we have to replace the usual derivatives by the covariant ones $\partial_\mu \to \partial_\mu + i2A_\mu$, where the factor 2 appears since the condensate is composed of two electrons. Due to the general gauge invariance principle, any shift of the gauge fields $A_{i=1,2} \to A_i - \partial_i\lambda$, $A_0 \to$

$A_0 - \partial_\tau \lambda$ has to be compensated by the phase of the field $\varphi \to \exp[-i2\lambda]\varphi$, which therefore must become complex. The phase must disappear again if the field is turned off, i.e., it must depend on the fields itself. On the other hand, the Aharonov-Bohm phase of the real field must obey

$$\frac{\Phi}{\phi_0} = n\pi, \tag{26}$$

with n being a natural number and ϕ_0 the elementary flux quantum, such that $\exp[i\Phi/\phi_0] = \pm 1$. The interlayer fractional quantum Hall effect measured in layered systems, cf. Refs. [19,20], suggests the possibility of phenomenological inclusion of the internal statistical vector potential, cf. Refs. [22,23,36]:

$$\mathcal{S}[a, A, \varphi] = \kappa\epsilon_{\mu\nu\rho} a_\mu \partial_\nu a_\rho + \tfrac{1}{2}|(\partial_\mu + i2a_\mu + i2A_\mu)\varphi|^2 + \tfrac{1}{4}(|\varphi|^2 - 1)^2, \tag{27}$$

where we absorbed ξ into the derivatives and neglect a constant term, which is not an integration variable and cancels by the same term in the normalization of a correlation function. The model looks like a relativistic extension of the ZHK model [23]. It is left to future activities to study the implications of these changes on the vortex formation in the model Eq. (27). The obvious minimum of the action Eq. (27) is given by the "self-dual" field configuration $|\varphi|^2 = 1$ and $a_\mu = -A_\mu$, in which the external gauge field is totally compensated by the Chern-Simons field. Correspondingly, the external magnetic field (i.e., the curl of A) is compensated by the internal field. The major difference from the ZHK model is that, since we start with the bosonic fields φ, we are not bound by the constraint for κ being fixed to $1/2\pi(2k+1)$ with integer k. In our case, there is no need to require the preservation of the anticommutation relations for the composite bosons. Because of the well- known deficiency of the phenomenological Chern-Simons theories, the value of κ should therefore be chosen to satisfy the experimental data and cannot in general be fixed by any microscopic reasoning [37].

Another significant difference is due to the fact that the curl of the statistical field is linked not to the particle density, but to the zeroth component of the current density. To see this we vary the action with respect to the a_0 component of the statistical gauge field and get

$$\begin{aligned} 0 &= 2\kappa\epsilon_{\mu\nu}\partial_\mu a_\nu - \frac{1}{i}\xi^2[\bar\varphi\mathcal{D}_0\varphi - \varphi\bar{\mathcal{D}}_0\bar\varphi] \\ &= 2\kappa b + 2J_0 + 4(a_0 + A_0)\rho, \end{aligned} \tag{28}$$

where $\rho = \bar\varphi\varphi$ and

$$J_0 = \frac{1}{2i}[\varphi\partial_\tau\bar\varphi - \bar\varphi\partial_\tau\varphi] = \rho\partial_\tau\theta, \tag{29}$$

with θ representing the phase of the field φ. A solution independent of external fields is given at the "self-dual point" $a_0 = -A_0$, which then leaves us with

$$\kappa b = -J_0, \tag{30}$$

where $b = \epsilon_{\mu\nu}\partial_\mu a_\nu$. This is the constraint condition of the relativistic model, which appears in place of the usual ZHK condition $\kappa b = -\rho$ [23]. As discussed in Ref. [38] (with reference to Refs. [39,40]) the integral over the whole space time of Eq. (30) relates the magnetic flux to the electric charge

$$\kappa\Phi = Q, \tag{31}$$

in a typical fashion for anions. Our aim is to clarify the structure of the filling factors from Eq. (30). At scales much larger than ξ the density of quasiparticles ρ should approach a uniform value, as suggested by the potential minimum of Eq. (27). Then integrating the current J_0 along the closed time contour should give

$$\oint_{|\tau|\gg 1} d\tau J_0 \approx \pi n\rho, \tag{32}$$

where the vorticity quantization is chosen in accord with the constraint condition Eq. (26). The same operation on the right-hand side must reduce the time dependent Chern-Simons magnetic field $b = \epsilon_{\mu\nu}\partial_\mu a_\nu$ to the time-independent flux density

$$\kappa\oint_{|\tau|\gg 1} d\tau b \approx \kappa B^{\rm CS} = -\kappa B^{\rm ext}, \tag{33}$$

where $B^{\rm ext}$ represents the external flux density and introduced after exploiting the "self-dual point" condition. Putting $\kappa = \pi k$ we, therefore, deduce the expression for the filling factor

$$\nu = \frac{\rho}{B^{\rm ext}} = \frac{k}{n}, \tag{34}$$

and, therefore, the anticipated expressions for the Hall conductivities

$$R_{xy} = \frac{1}{\sigma_0}\frac{1}{\nu} = \frac{1}{\sigma_0}\frac{n}{k}, \tag{35}$$

with the universal conductivity $\sigma_0 = e^2/2\pi\hbar$. As it was pointed out before, while n is fixed to be an integer number, k represents a free parameter of the Chern-Simons theory. In general, $1/k$ is related to the total angular momentum of the system and appears in the exponent of the corresponding Laughlin state [41]. The ratios n/k are read off the experimental data in a form of a rational numbers, e.g., Ref. [19]. We discuss the physical consequences of Eq. (34) at the end of the Conclusions.

VI. CONCLUSIONS

One of the unresolved problems in our previous work Ref. [15] was the solid justification of the emergent staggered order parameter. This order parameter is hard to anticipate from the superficial inspection of the original Hubbard-like interaction term, which is given in terms of electronic densities, which dwell in opposite layers and feel each other across the interlayer gap through the Coulomb repulsion. Here we deliver a conclusive argument employing a combination of the Fierz-like transformations and renormalization group analysis. The first suggests the existence of a particular representation of the original interaction between densities laying in different layers in terms of composite interacting objects, which are formed from the particles from both layers. However, there are several species of such composite objects which are described in terms of different Pauli channels. Does the model take both Dirac particles in each layer into account, then the number of channels increases quadratically. *A priori* it is not clear which of the channels should be dominant and one can anticipate a number of possible order parameters. The decisive insight is gained with the help of the RG arguments.

From the theory of phase transitions it is known that the realistic physical interactions which govern them usually differ from the simple phenomenological ansaetze we use in the modeling. The RG provides for a formal (even if phenomenological) tool to select, which of the interactions becomes dominant in the energy area of interest. This is the essential idea of what is called the "emergency principle". The result of Eq. (17) reflects just that: while all coupling parameters start running at the same bare value, the coupling parameter in the σ_3 channel grows faster than the competitors and develops a Landau pole. The related singularity signals, that (1) the σ_3 channel is in fact the physical interaction responsible for the pairing; (2) the perturbative approach breaks down and we must employ self-consistent mean-field approaches instead. The scale of the Landau pole can also be approximately extracted from the mean-field equation for the order parameter. Hence, we interpret the Landau pole as the manifestation of transition into the paired phase and the emerging staggered order as the dominant pairing mechanism.

In order to analyze the consequences resulting from the interaction between the condensate and external magnetic field it is not sufficient to restrict the considerations only to the mean-field equations. Instead what we need is detailed information about the structure of the effective action, which describes the behavior of fluctuations of the order parameter. This task is similar in nature to the usual Ginzburg-Landau program of the superconductivity, which has been also applied to the fractional quantum Hall effects for simple filling factors [36]. To clarify the structure of the effective action which governs the behavior of fluctuations we perform an expansion in powers of the inverse superconducting gap parameter combined with the gradient expansion in the quadratic part. The main difference in contrast to the conventional Ginzburg-Landau program is that the low-energy effective action for the fluctuations of the order parameter turns out to be Lorentzian invariant; that is the classical equation of motion of the fluctuations appear to be not a type of Schrödinger equation but rather a Klein - Gordon equation. This simple fact has significant consequences for the behavior of the condensate in the magnetic field.

Since the interlayer condensate is not electrically neutral but possesses a charge twice the value of the single electron it must feel the presence of the background magnetic field and behave according to the common understanding of the quantum Hall physics. In particular the composite particles formed by the attachment of flux quanta to the charged fluctuations of the superconducting order parameter must appear. Technically, the flux attachment is caught by the introduction of the Chern-Simons fields, which couples minimally, e.g., via the covariant derivative to the condensate. The specifics of our model as compared to the ZHK model [22,23] is due to its Lorentzian invariance, which results in different constraint conditions. For instance, because of this the time component of the curl of the Chern-Simons gauge field is linked to the time component of the current and not to the density of particles. Upon the time integration, this constraint condition boils down to the relationship between the external magnetic field and particles density, that is the filling factor, which is principally different than that of the ZHK model. It is of great interest to study the Chern-Simons vortex phase of the model Eq. (27) and the response of the system in the corresponding phase. The results of these investigations will be reported in a separate publication.

Chern-Simons theories of the fractional quantum Hall effects represent merely a phenomenological description of the phenomenon, as do the semimicroscopic approaches based on the analysis of the Laughlin states. Both are related to each other and the exponent in the holomorphic term of the Laughlin wave function represents the inverse of the factor k in front of the respective Chern-Simons term [37]. In simple cases (e.g., □-function potential) the exponents are related to the total angular momentum of the physical state, we refer, for instance, to a thorough discussion in Fradkins book [41]. In general, though, it is not clear what fixes those numbers. The known sequences, i.e., Jain sequences [21], do not capture all fractional Hall states observed so far. In practice, the filling factors of experimentally observed plateaus are extracted as ratio total flux/elementary flux, for which then an appropriate rational number is sought. A glimpse at the experimental data, e.g., presented in Fig. 1 in Ref. [19], reveals how cumbersome this task might be. Here, a large portion of clearly visible plateaus remained unidentified. Upon completing the identification task, these numbers are brought into connection with the related Laughlin states and Chern-Simons theories [22,37]. Hence, Eq. (34) includes all fractional filling factors reportedly measured in Ref. [20]. For more detailed discussions of the role and predictable power of phenomenological approaches we refer to a number of excellent reviews and lectures on the topic in Refs. [41–44].

ACKNOWLEDGMENTS

This work was partially supported by the Agencia Nacional de Investigacion de España through Grant No. PCI2021-122057-2B and partially performed at the Madrid Institute for Advanced Studies IMDEA Nanosciencia. Insightful exchange on the topic with Professor F. Guinea and Dr. P. Pantanleón are gratefully acknowledged. Early collaboration with Professor K. Ziegler and Professor Y. Lozovik is gratefully appreciated. The author expresses his gratitude to Max-Planck Institute for Physics of Complex Systems MPIPKS Dresden for the hospitality and support through the Visitors Program at initial stages of this work.

APPENDIX A: DENSITY-DENSITY INTERACTION REPRESENTATION IN THE INTERLAYER BASIS

In the subsequent chapters we explain explicitly the representation of the initial interaction between densities in each individual layer in the interlayer basis for several cases.

1. The reparametrization of the effective Hubbard interaction on the lattice

We start with the effective Hubbard interaction for two-component fermion on each lattice site introduced in Ref. [15]

without proof

$$\frac{1}{2}n_\uparrow n_\downarrow = \frac{1}{2}(n_\uparrow + n_\downarrow) - \frac{1}{8}\sum_{\mu=0}^{3}[(\hat{c}_\uparrow^\dagger\sigma_\mu\hat{c}_\downarrow)(\hat{c}_\downarrow^\dagger\sigma_\mu\hat{c}_\uparrow) + (\hat{c}_\downarrow^\dagger\sigma_\mu\hat{c}_\uparrow)(\hat{c}_\uparrow^\dagger\sigma_\mu\hat{c}_\downarrow)], \tag{A1}$$

where the density operators $n_s = c_s^\dagger c_s + d_s^\dagger d_s$, and the spinors $\hat{c}_s = (c_s, d_s)^{\mathrm{T}}$ are composed of fermions related to each sublattice, i.e., $\hat{c}_{1s} = c_s$ and $\hat{c}_{2s} = d_s$. The usual anticommutation relations for the components of the spinors

$$\{\hat{c}_{is}^\dagger, \hat{c}_{i's'}\} = \delta_{ii'}\delta_{ss'}, \tag{A2}$$

together with the Pauli prohibition relations

$$\hat{c}_{is}^\dagger\hat{c}_{is}^\dagger = 0 = \hat{c}_{is}\hat{c}_{is}, \tag{A3}$$

means that the normal ordering of the operators on the left-hand side in Eq. (A1) does not produce any density monomials:

$$n_\uparrow n_\downarrow = c_\uparrow^\dagger c_\downarrow^\dagger c_\downarrow c_\uparrow + c_\uparrow^\dagger d_\downarrow^\dagger d_\downarrow c_\uparrow + d_\uparrow^\dagger c_\downarrow^\dagger c_\downarrow d_\uparrow + d_\uparrow^\dagger d_\downarrow^\dagger d_\downarrow d_\uparrow. \tag{A4}$$

In the functional integral it allows the direct introduction of the Grassmann coherent states $|\varphi_\uparrow, \varphi_\downarrow, \chi_\uparrow, \chi_\downarrow\rangle$, and direct replacement of the fermionic second quantization operators by the respective Grassmann fields. Therefore, the structure of the interaction terms remains the same also in the action of the functional integral:

$$n_\uparrow n_\downarrow \to (\psi_\uparrow^\dagger\psi_\uparrow)(\psi_\downarrow^\dagger\psi_\downarrow), \tag{A5}$$

where $\psi_s = (\varphi_s, \chi_s)^{\mathrm{T}}$. Next, we consider the right-hand side of Eq. (A1). First term under the sum over μ reads

$$\sum_{\mu=0}^{3}(\hat{c}_\uparrow^\dagger\sigma_\mu\hat{c}_\downarrow)(\hat{c}_\downarrow^\dagger\sigma_\mu\hat{c}_\uparrow) = \hat{c}_{s\uparrow}^\dagger\sigma_\mu^{ss'}\hat{c}_{s'\downarrow}\,\hat{c}_{p\downarrow}^\dagger\sigma_\mu^{pp'}\hat{c}_{p'\uparrow}, \tag{A6}$$

where we now employ the Einstein summation convection (the repeated symbols is summed over) for all symbols, i.e., also μ. The nonzero elements of the Pauli matrices are

$$\begin{aligned}\sigma_0^{11} &= \sigma_0^{22} = 1;\ \ \sigma_3^{11} = -\sigma_3^{22} = 1;\\ \sigma_1^{12} &= \sigma_1^{21} = 1;\ \ \sigma_2^{12} = -\sigma_0^{21} = -i.\end{aligned} \tag{A7}$$

This implies for Eq. (A6)

$$\begin{aligned}\hat{c}_{s\uparrow}^\dagger\sigma_\mu^{ss'}\hat{c}_{s'\downarrow}\,\hat{c}_{p\downarrow}^\dagger\sigma_\mu^{pp'}\hat{c}_{p'\uparrow} &= \underbrace{[c_\uparrow^\dagger c_\downarrow + d_\uparrow^\dagger d_\downarrow][c_\downarrow^\dagger c_\uparrow + d_\downarrow^\dagger d_\uparrow]}_{\mu=0}\\ &+ \underbrace{[c_\uparrow^\dagger c_\downarrow - d_\uparrow^\dagger d_\downarrow][c_\downarrow^\dagger c_\uparrow - d_\downarrow^\dagger d_\uparrow]}_{\mu=3} \qquad (\text{A8})\\ &+ \underbrace{[c_\uparrow^\dagger d_\downarrow + d_\uparrow^\dagger c_\downarrow][c_\downarrow^\dagger d_\uparrow + d_\downarrow^\dagger c_\uparrow]}_{\mu=1}\\ &- \underbrace{[c_\uparrow^\dagger d_\downarrow - d_\uparrow^\dagger c_\downarrow][c_\downarrow^\dagger d_\uparrow - d_\downarrow^\dagger c_\uparrow]}_{\mu=2} \qquad (\text{A9})\\ &= 2[c_\uparrow^\dagger c_\uparrow + d_\uparrow^\dagger d_\uparrow][c_\downarrow c_\downarrow^\dagger + d_\downarrow d_\downarrow^\dagger]\\ &= 4n_\uparrow - 2n_\uparrow n_\downarrow. \qquad (\text{A10})\end{aligned}$$

Analogously we get for the second term

$$\sum_{\mu=0}^{3}(\hat{c}_\downarrow^\dagger\sigma_\mu\hat{c}_\uparrow)(\hat{c}_\uparrow^\dagger\sigma_\mu\hat{c}_\downarrow) = 4n_\downarrow - 2n_\uparrow n_\downarrow. \tag{A11}$$

Inserting both Eqs. (A8) and (A11) into Eq. (A1) finalizes the proof. It can be easily generalized to extended interactions.

The results are slightly different when working with Grassmann fields. Because of the Grassmann numbers algebra $\chi_i\chi_j = -\chi_j\chi_i$ (for a generic Grassmann number χ), similar evaluations do not produce any density monomials. Furtheremore, both terms under the sum on the right-hand side of Eq. (A1) turn out to be identical. One, therefore, directly gets to the equality

$$\tfrac{1}{2}(\psi_\uparrow^\dagger\psi_\uparrow)(\psi_\downarrow^\dagger\psi_\downarrow) = -\tfrac{1}{4}(\psi_\uparrow^\dagger\sigma_\mu\psi_\downarrow)(\psi_\downarrow^\dagger\sigma_\mu\psi_\uparrow), \tag{A12}$$

which is supposed to be the starting action for the renormalization group flow. Introducing the counter terms in each channel in the form

$$-\tfrac{1}{4}(Z_\mu - 1)(\psi_\uparrow^\dagger\sigma_\mu\psi_\downarrow)(\psi_\downarrow^\dagger\sigma_\mu\psi_\uparrow), \tag{A13}$$

and consequently the flowing interactions $g_\mu = gZ_\mu$ we finally get to the action Eq. (11).

2. Interaction for two Dirac cones

In the case where both cones are accounted for as in Eq. (5) the calculations are similar. Here we use the Grassmann fields formalism. The bispinors in the layer s read $\Psi_s = (\psi_{as}, \psi_{bs})^{\mathrm{T}}$, where a and b refer to each of two Dirac cones. The product of density bilineals on the left-hand side of Eq. (5) is

$$(\Psi_\uparrow^\dagger\Psi_\uparrow)(\Psi_\downarrow^\dagger\Psi_\downarrow) = \sum_{\alpha=a,b}\sum_{\beta=a,b}(\psi_{\alpha\uparrow}^\dagger\psi_{\alpha\uparrow})(\psi_{\beta\downarrow}^\dagger\psi_{\beta\downarrow}). \tag{A14}$$

For the consideration on the right-hand side of Eq. (5) we first write out the sum over μ using Eq. (A7) (and skipping the constant factors for the time being)

$$\begin{aligned}&(\Psi_\uparrow^\dagger\Sigma_{\mu\nu}\Psi_\downarrow)(\Psi_\downarrow^\dagger\Sigma_{\mu\nu}\Psi_\uparrow)\\ &= \underbrace{[\psi_{a\uparrow}^\dagger\sigma_\nu\psi_{a\downarrow} + \psi_{b\uparrow}^\dagger\sigma_\nu\psi_{b\downarrow}][\psi_{a\downarrow}^\dagger\sigma_\nu\psi_{a\uparrow} + \psi_{b\downarrow}^\dagger\sigma_\nu\psi_{b\uparrow}]}_{\mu=0} \qquad (\text{A15})\\ &+ \underbrace{[\psi_{a\uparrow}^\dagger\sigma_\nu\psi_{a\downarrow} - \psi_{b\uparrow}^\dagger\sigma_\nu\psi_{b\downarrow}][\psi_{a\downarrow}^\dagger\sigma_\nu\psi_{a\uparrow} - \psi_{b\downarrow}^\dagger\sigma_\nu\psi_{b\uparrow}]}_{\mu=3} \qquad (\text{A16})\\ &+ \underbrace{[\psi_{a\uparrow}^\dagger\sigma_\nu\psi_{b\downarrow} + \psi_{b\uparrow}^\dagger\sigma_\nu\psi_{a\downarrow}][\psi_{a\downarrow}^\dagger\sigma_\nu\psi_{b\uparrow} + \psi_{b\downarrow}^\dagger\sigma_\nu\psi_{a\uparrow}]}_{\mu=1} \qquad (\text{A17})\\ &- \underbrace{[\psi_{a\uparrow}^\dagger\sigma_\nu\psi_{b\downarrow} - \psi_{b\uparrow}^\dagger\sigma_\nu\psi_{a\downarrow}][\psi_{a\downarrow}^\dagger\sigma_\nu\psi_{b\uparrow} - \psi_{b\downarrow}^\dagger\sigma_\nu\psi_{a\uparrow}]}_{\mu=2} \qquad (\text{A18})\\ &= 2\sum_{\alpha,\beta=a,b}(\psi_{\alpha\uparrow}^\dagger\sigma_\nu\psi_{\beta\downarrow})(\psi_{\beta\downarrow}^\dagger\sigma_\nu\psi_{\alpha\uparrow}). \qquad (\text{A19})\end{aligned}$$

Further, each of the elements on the right-hand side

$$
\begin{aligned}
&2(\psi^\dagger_{\alpha\uparrow}\sigma_\nu\psi_{\beta\downarrow})(\psi^\dagger_{\beta\downarrow}\sigma_\nu\psi_{\alpha\uparrow})\\
&= 2\underbrace{[\psi^\dagger_{1\alpha\uparrow}\psi_{1\beta\downarrow}+\psi^\dagger_{2\alpha\uparrow}\psi_{2\beta\downarrow}][\psi^\dagger_{1\beta\downarrow}\psi_{1\alpha\uparrow}+\psi^\dagger_{2\beta\downarrow}\psi_{2\alpha\uparrow}]}_{\nu=0} \qquad \text{(A20)}\\
&+2\underbrace{[\psi^\dagger_{1\alpha\uparrow}\psi_{1\beta\downarrow}-\psi^\dagger_{2\alpha\uparrow}\psi_{2\beta\downarrow}][\psi^\dagger_{1\beta\downarrow}\psi_{1\alpha\uparrow}-\psi^\dagger_{2\beta\downarrow}\psi_{2\alpha\uparrow}]}_{\nu=3} \qquad \text{(A21)}\\
&+2\underbrace{[\psi^\dagger_{1\alpha\uparrow}\psi_{2\beta\downarrow}+\psi^\dagger_{2\alpha\uparrow}\psi_{1\beta\downarrow}][\psi^\dagger_{1\beta\downarrow}\psi_{2\alpha\uparrow}+\psi^\dagger_{2\beta\downarrow}\psi_{1\alpha\uparrow}]}_{\nu=1} \qquad \text{(A22)}\\
&-2\underbrace{[\psi^\dagger_{1\alpha\uparrow}\psi_{2\beta\downarrow}-\psi^\dagger_{2\alpha\uparrow}\psi_{1\beta\downarrow}][\psi^\dagger_{1\beta\downarrow}\psi_{2\alpha\uparrow}-\psi^\dagger_{2\beta\downarrow}\psi_{1\alpha\uparrow}]}_{\nu=2} \qquad \text{(A23)}\\
&= 4\underline{\psi^\dagger_{1\alpha\uparrow}\psi_{1\beta\downarrow}\psi^\dagger_{1\beta\downarrow}\psi_{1\alpha\uparrow}}+4\underline{\underline{\psi^\dagger_{2\alpha\uparrow}\psi_{2\beta\downarrow}\psi^\dagger_{2\beta\downarrow}\psi_{2\alpha\uparrow}}} \qquad \text{(A24)}\\
&+4\underline{\underline{\psi^\dagger_{1\alpha\uparrow}\psi_{2\beta\downarrow}\psi^\dagger_{2\beta\downarrow}\psi_{1\alpha\uparrow}}}+4\underline{\psi^\dagger_{2\alpha\uparrow}\psi_{1\beta\downarrow}\psi^\dagger_{1\beta\downarrow}\psi_{2\alpha\uparrow}} \qquad \text{(A25)}\\
&= -4(\psi^\dagger_{\alpha\uparrow}\psi_{\alpha\uparrow})(\psi^\dagger_{\beta\downarrow}\psi_{\beta\downarrow}). \qquad \text{(A26)}
\end{aligned}
$$

Hence

$$
\begin{aligned}
&-\frac{1}{4}(\Psi^\dagger_\uparrow\Sigma_{\mu\nu}\Psi_\downarrow)(\Psi^\dagger_\downarrow\Sigma_{\mu\nu}\Psi_\uparrow)\\
&= \sum_{\alpha,\beta=a,b}(\psi^\dagger_{\alpha\uparrow}\psi_{\alpha\uparrow})(\psi^\dagger_{\beta\downarrow}\psi_{\beta\downarrow}) = (\Psi^\dagger_\uparrow\Psi_\uparrow)(\Psi^\dagger_\downarrow\Psi_\downarrow), \qquad \text{(A27)}
\end{aligned}
$$

where we used Eq. (A14). This proofs Eq. (5).

3. The analogon of Eq. (7) for the model with two Dirac cones per layer

For the model with two Dirac cones with different chirality per layer the initial action reads

$$
\mathcal{S} = \sum_{s=\uparrow\downarrow}\Psi^\dagger_s\cdot[\partial_\tau\Sigma_{00}+H_0]\Psi_s - \frac{g}{8}(\Psi^\dagger_\uparrow\Sigma_{\mu\nu}\Psi_\downarrow)(\Psi^\dagger_\downarrow\Sigma_{\mu\nu}\Psi_\uparrow). \qquad \text{(A28)}
$$

The difference in the chirality of the cones is reflected in the form of the Hamiltonian H_0

$$
H_0 = i\partial_x\Sigma_{01} + i\partial_y\Sigma_{32}. \qquad \text{(A29)}
$$

The mean-field approximation

$$
\Delta_{\mu\nu} = -\frac{g}{8}\langle\Psi^\dagger_\uparrow\Sigma_{\mu\nu}\Psi_\downarrow\rangle \qquad \text{(A30)}
$$

leads then to the Bogoliubov–de Gennes action

$$
\mathcal{S}_{\mathrm{BdG}} = \begin{pmatrix}\Psi_\uparrow\\ \Psi_\downarrow\end{pmatrix}^{\mathrm{T}}\cdot\begin{pmatrix}\partial_\tau\Sigma_{00}+H_0 & \Delta_{\mu\nu}\\ \Delta^*_{\mu\nu} & \partial_\tau\Sigma_{00}+H_0\end{pmatrix}\begin{pmatrix}\Psi_\uparrow\\ \Psi_\downarrow\end{pmatrix}, \qquad \text{(A31)}
$$

with the matrix representing the inverse Greens function. Order parameters which correspond to the stable phase should allow for the inversion of the Greens function without producing any singularities. This is given if the components of the order parameters anticommute mutually and with the Hamiltonian H_0. This restricts the possible candidates to

$$
\Delta_1\Sigma_{22} + \Delta_2\Sigma_{12}, \qquad \text{(A32)}
$$

since indeed

$$
\{\Sigma_{22},\Sigma_{12}\} = 0, \quad \{\Sigma_{12},H_0\} = 0, \quad \{\Sigma_{22},H_0\} = 0. \qquad \text{(A33)}
$$

These constraints lead to the similar equations for Δ_1 and Δ_2

$$
\Delta_1 = \frac{g}{8}\mathrm{tr}\Sigma_{22}\int\frac{d^3Q}{(2\pi)^3}\frac{\Delta_1\Sigma_{22}+\Delta_2\Sigma_{12}}{Q^2+|\Delta|^2}, \qquad \text{(A34)}
$$

$$
\Delta_2 = \frac{g}{8}\mathrm{tr}\Sigma_{12}\int\frac{d^3Q}{(2\pi)^3}\frac{\Delta_1\Sigma_{22}+\Delta_2\Sigma_{12}}{Q^2+|\Delta|^2}, \qquad \text{(A35)}
$$

where $|\Delta|^2 = \Delta_1^*\Delta_1 + \Delta_2^*\Delta_2$. Both equations lead further to

$$
1 = \frac{g}{2}\int^\Lambda\frac{d^2q}{(2\pi)^2}\int\frac{dq_0}{2\pi}\frac{1}{q_0^2+q^2+|\Delta|^2}, \qquad \text{(A36)}
$$

which is formally similar to Eq. (10) for the one-cone model. It only fixes $|\Delta|$ but not each component individually. This allows one to assume them to be real and equal to each other.

APPENDIX B: DERIVATION AND EVALUATION OF THE RENORMALIZATION GROUP EQUATIONS

In this Appendix we consider possible perturbative processes below the pairing transition. This phase is characterized by the absence of the off-diagonal elements in the Greens function. In particular this means that only fields from the same layer correlate and can be contracted

$$
\langle\psi_{X\uparrow}\psi^\dagger_{X'\uparrow}\rangle = G(X,X') = \langle\psi_{X\downarrow}\psi^\dagger_{X'\downarrow}\rangle, \qquad \text{(B1)}
$$

$$
\langle\psi_{X\uparrow}\psi^\dagger_{X'\downarrow}\rangle = 0 = \langle\psi_{X\downarrow}\psi^\dagger_{X'\uparrow}\rangle. \qquad \text{(B2)}
$$

The interaction term $(\psi^\dagger_\uparrow\sigma_\mu\psi_\downarrow)(\psi^\dagger_\downarrow\sigma_\mu\psi_\uparrow)$ has the following diagrammatic form:

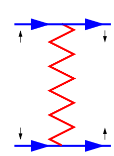
,

where the ingoing leg denotes the field ψ and the outgoing the field $\psi^\dagger$. When evaluating second-order perturbative processes we need only those which recover the same topology of the interaction term.

1. Diagrammatics of the perturbative processes to first- and second-order

Generally, there two topological classes of first-order perturbative processes for the fermionic self-energy:

(1a). The first order bubble diagram

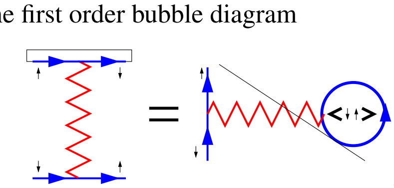

This contribution requires contracting fields from different layers and is therefore zero.

(1b). The first-order rainbow diagram

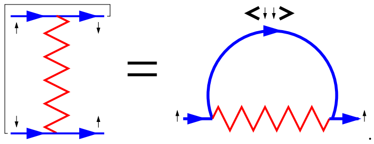

The contribution from this diagram vanishes by angular integration.

In the second-order of perturbative expansion there are in general four topological processes which renormalize the interaction term. These are

(2a). The "ladder" diagram

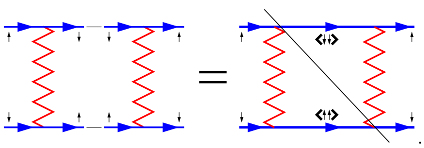

This diagram has the form $(\psi_\downarrow^\dagger\sigma_\mu\psi_\downarrow)(\psi_\uparrow^\dagger\sigma_\mu\psi_\uparrow)$, which is different from the original interaction. This contribution does not renormalize the bare interaction but creates a higher-order interaction term.

(2b). The "fan" diagram

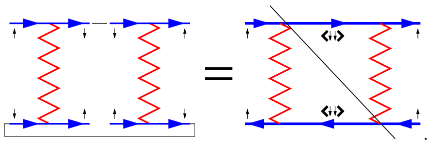

This processes creates the subordinate interaction of the type $(\psi_\uparrow^\dagger\sigma_\mu\psi_\uparrow)(\psi_\uparrow^\dagger\sigma_\mu\psi_\uparrow)$ and again does not renormalize the bare interaction.

(2c). The "penguin" diagram

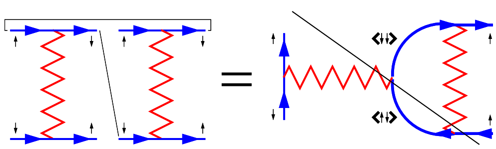

This diagram requires contracting fields from different layers and is therefore zero.

(2d). The "bubble" diagram

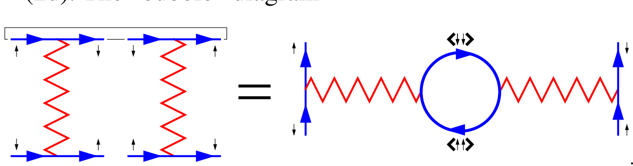

This contribution recovers correctly the topology of the bare interaction term. This is the only process which gives the renormalization of the original interaction. In analytical form this process leads to Eq. (14) and is evaluated in Appendix B 2 for all channels.

2. Evaluation of the RG equation Eq. (14)

In this Appendix we evaluate the master RG equation Eq. (14) for different channels.

(1) $\mu = 0$, this channel does not get renormalized to the leading order, since it vanishes after the frequency integration from infinity to infinity:

$$\begin{aligned}
\mathrm{Tr}\int \frac{dq_0}{2\pi} G(Q)\sigma_0 G(Q)\sigma_0 &= \int \frac{dq_0}{2\pi}\frac{1}{\left[q_0^2+q^2\right]^2}\mathrm{Tr}\{[q\cdot\sigma - iq_0\sigma_0][q\cdot\sigma - iq_0\sigma_0]\} \\
&\sim \int \frac{dq_0}{2\pi}\frac{q^2-q_0^2}{\left[q_0^2+q^2\right]^2}.
\end{aligned} \tag{B3}$$

The numerator is replaced by the derivatives to the auxiliary variable α

$$\begin{aligned}
\int \frac{dq_0}{2\pi}\frac{q^2-q_0^2}{\left[q_0^2+q^2\right]^2} &= \frac{\partial}{\partial\alpha}\bigg|_{\alpha=1}\int\frac{dq_0}{2\pi}\left[\frac{1}{\alpha q_0^2+q^2} - \frac{1}{q_0^2+\alpha q^2}\right].
\end{aligned} \tag{B4}$$

The integration goes from $-\infty$ to $+\infty$, which enables us to rescale the integration variable in the first term as $q_0 \to q_0/\sqrt{\alpha}$ and to carry out the integral by the Cauchy theorem

$$\begin{aligned}
\int\frac{dq_0}{2\pi}\left[\frac{1}{\alpha q_0^2+q^2} - \frac{1}{q_0^2+\alpha q^2}\right] &= \int\frac{dq_0}{2\pi}\left[\frac{1}{\sqrt{\alpha}}\frac{1}{q_0^2+q^2} - \frac{1}{q_0^2+\alpha q^2}\right] \\
&= \frac{1}{\sqrt{\alpha}}\frac{1}{2q} - \frac{1}{2\sqrt{\alpha}q} = 0.
\end{aligned} \tag{B5}$$

Hence, this channel remains invariant under the RG transformation to one-loop order and can be neglected in comparison to the more relevant channels.

(2) $\mu = 1, 2$. The important detail for the further computations concerns the behavior of the spatial momenta under the trace and angular integration. We carry out the calculations for $\mu = 1$, the other case is absolutely analogous:

$$\begin{aligned}
\int_0^{2\pi}\frac{d\phi}{2\pi}\, q\cdot\sigma\sigma_1 q\cdot\sigma\sigma_1 &= \int_0^{2\pi}\frac{d\phi}{2\pi}\, q_i q_j\,\sigma_i\sigma_1\sigma_j\sigma_1 \\
&= \frac{1}{2}q^2\delta_{ij}\sigma_i\sigma_1\sigma_j\sigma_1\int_0^{2\pi}\frac{d\phi}{2\pi}.
\end{aligned} \tag{B6}$$

The product of Pauli matrices becomes zero

$$\sigma_i\sigma_1\sigma_i\sigma_1 = \sigma_1\sigma_1\sigma_1\sigma_1 + \sigma_2\sigma_1\sigma_2\sigma_1 = \sigma_0 - \sigma_0 = 0. \tag{B7}$$

The remaining parts give the following result:

$$\begin{aligned}
\tilde{g}_{1,2} &= -\frac{g_{1,2}^2}{16}\mathrm{Tr}\int\frac{d^3Q}{(2\pi)^3}G(Q)\sigma_{1,2}G(Q)\sigma_{1,2} \\
&= -\frac{g_{1,2}^2}{8}\int\frac{d^3Q}{(2\pi)^3}\frac{-q_0^2}{\left[q_0^2+q^2\right]^2}.
\end{aligned} \tag{B8}$$

The evaluation with the help of auxiliary variable as in the previous example gives

$$\tilde{g}_{1,2} = \frac{g_{1,2}^2}{32}\int^{\Lambda}\frac{d^2q}{(2\pi)^2}\frac{1}{q} = \frac{g_{1,2}^2}{32}\frac{\Lambda_0-\Lambda}{2\pi}. \tag{B9}$$

For the thin momentum shell we can express the lower cutoff as $\Lambda \sim \Lambda_0 e^{-\ell} \sim \Lambda_0(1-\ell)$, such that the correction becomes

$$\tilde{g}_{1,2} = \frac{g_{1,2}^2}{32}\frac{\Lambda_0}{2\pi}\ell, \tag{B10}$$

which upon rising into the exponent yields the renormalization correction for these channels

$$\bar{g}_{1,2} = g_{1,2} + \frac{g_{1,2}^2}{32}\frac{\Lambda_0}{2\pi}\ell, \tag{B11}$$

and correspondingly the differential RG flow equation Eq. (15).

(3) $\mu = 3$. The reasoning here is analogous to the previous case:

$$\begin{aligned}\mathrm{Tr}\int_0^{2\pi}\frac{d\phi}{2\pi}\, q\cdot\sigma\sigma_3 q\cdot\sigma\sigma_3 &= \mathrm{Tr}\int_0^{2\pi}\frac{d\phi}{2\pi}\, q_i q_j\,\sigma_i\sigma_3\sigma_j\sigma_3\\ &= \frac{1}{2}q^2\mathrm{Tr}\sigma_i\sigma_3\sigma_i\sigma_3 = -q^2,\end{aligned} \tag{B12}$$

the sign is because σ_3 anticommutes with both $\sigma_{1,2}$. Therefore, the numerator becomes $-q_0^2-q^2$, which then cancels one power in the denominator. The result becomes

$$\begin{aligned}\tilde{g}_3 &= -\frac{g_3^2}{16}\mathrm{Tr}\int\frac{d^3Q}{(2\pi)^3}G(Q)\sigma_3 G(Q)\sigma_3\\ &= \frac{g_3^2}{8}\int\frac{d^3Q}{(2\pi)^3}\frac{1}{q_0^2+q^2} = \frac{g_3^2}{16}\int^{\Lambda}\frac{d^2q}{(2\pi)^2}\frac{1}{q} = \frac{g_3^2}{16}\frac{\Lambda_0-\Lambda}{2\pi},\end{aligned} \tag{B13}$$

i.e., twice the value of $g_{1,2}$. In differential form the RG equation becomes Eq. (15).

APPENDIX C: LOOP EXPANSION OF THE ACTION EQ. (23)

Shifting the Hubbard-Stratonovich fields in Eq. (23) by the pairing condensate $\vec{\mathcal{Q}} \to \vec{\Delta} + \vec{\mathcal{Q}}$, the shifted action becomes

$$\begin{aligned}\mathcal{S}[\mathcal{Q}] &= \frac{4}{g}(\vec{\Delta}\cdot\vec{\Delta} + 2\vec{\Delta}\cdot\vec{\mathcal{Q}} + \vec{\mathcal{Q}}\cdot\vec{\mathcal{Q}}) - \mathrm{tr}\log[G^{-1}]\\ &\quad - \mathrm{tr}\log[1 + G\vec{\mathcal{Q}}\cdot\hat{\Sigma}],\end{aligned} \tag{C1}$$

where the propagator in the condensed phase is $G^{-1} = G_0^{-1} + \vec{\Delta}\cdot\hat{\Sigma}$. The minimization of the $\mathcal{Q}$-independent term (the vacuum energy) yields the saddle-point equations identical with Eq. (9)

$$\frac{2}{g} = \int\frac{d^3Q}{(2\pi)^3}\frac{1}{Q^2+\Delta^2}, \tag{C2}$$

where $\Delta = |\vec{\Delta}|$, and guarantees for the vanishing of all terms in the action, which appear to the linear order in $\mathcal{Q}$. The expansion of the log term in the action reads

$$\begin{aligned}\mathrm{tr}\log[1+G\vec{\mathcal{Q}}\cdot\hat{\Sigma}] &= \mathrm{tr}(G\vec{\mathcal{Q}}\cdot\hat{\Sigma}) - \tfrac{1}{2}\mathrm{tr}(G\vec{\mathcal{Q}}\cdot\hat{\Sigma})^2\\ &\quad + \tfrac{1}{3}\mathrm{tr}(G\vec{\mathcal{Q}}\cdot\hat{\Sigma})^3 - \tfrac{1}{4}\mathrm{tr}(G\vec{\mathcal{Q}}\cdot\hat{\Sigma})^4\cdots.\end{aligned} \tag{C3}$$

Dropping linear terms we get

$$\begin{aligned}\mathcal{S}[\mathcal{Q}] &= \frac{4}{g}\vec{\mathcal{Q}}\cdot\vec{\mathcal{Q}} + \frac{1}{2}\mathrm{tr}(G\vec{\mathcal{Q}}\cdot\hat{\Sigma})^2\\ &\quad - \frac{1}{3}\mathrm{tr}(G\vec{\mathcal{Q}}\cdot\hat{\Sigma})^3 + \tfrac{1}{4}\mathrm{tr}(G\vec{\mathcal{Q}}\cdot\hat{\Sigma})^4.\end{aligned} \tag{C4}$$

With the help of the saddle-point equation Eq. (C2), the quadratic part becomes to the leading order in the gradient expansion

$$\mathcal{S}^{(2)}[\mathcal{Q}] = \vec{\mathcal{Q}}\cdot M^{-1}\vec{\mathcal{Q}}, \tag{C5}$$

where the elements of the matrix M are

$$M_{11} = \frac{\Delta_1^2}{2\pi\Delta} + \frac{2\Delta^2+\Delta_2^2}{24\pi\Delta^3}P^2, \tag{C6}$$

$$M_{12} = \frac{\Delta_1\Delta_2}{2\pi\Delta} - \frac{\Delta_1\Delta_2}{24\pi\Delta^3}P^2 = M_{21}, \tag{C7}$$

$$M_{22} = \frac{\Delta_2^2}{2\pi\Delta} + \frac{2\Delta^2+\Delta_1^2}{24\pi\Delta^3}P^2, \tag{C8}$$

$P^2 = p_0^2 + p^2$. Of two eigenvalues of the matrix M one is gapless (Goldstone mode, E_{G}) and the other gaped (Higgs mode, E_{H})

$$E_{\mathrm{G}} = \frac{P^2}{8\pi\Delta},\quad E_{\mathrm{H}} = \frac{\Delta}{2\pi} + \frac{P^2}{12\pi\Delta}. \tag{C9}$$

The diagonalization of the matrix M^{-1} is done by the orthogonal and self-inverse transformation

$$\mathbf{U} = \frac{1}{\Delta}\begin{pmatrix}-\Delta_1 & -\Delta_2\\ -\Delta_2 & \Delta_1\end{pmatrix}. \tag{C10}$$

The fields $\mathcal{Q}$ transform into diagonal representation $\mathcal{C}$ as

$$\mathcal{Q}_1 = -\frac{\Delta_1}{\Delta}\mathcal{C}_1 - \frac{\Delta_2}{\Delta}\mathcal{C}_2,\quad \mathcal{Q}_2 = -\frac{\Delta_2}{\Delta}\mathcal{C}_1 + \frac{\Delta_1}{\Delta}\mathcal{C}_2. \tag{C11}$$

In the $\mathcal{C}$ basis, the quadratic action is

$$\mathcal{S}^{(2)} = \mathcal{C}_1\cdot E_H\mathcal{C}_1 + \mathcal{C}_2\cdot E_G\mathcal{C}_2. \tag{C12}$$

The cubic part of the action follows as

$$\begin{aligned}-\tfrac{1}{3}\mathrm{tr}(G\vec{\mathcal{Q}}\cdot\hat{\Sigma})^3 &= -\alpha_{111}\mathcal{Q}_1^3 - \alpha_{112}\mathcal{Q}_1^2\mathcal{Q}_2\\ &\quad - \alpha_{122}\mathcal{Q}_1\mathcal{Q}_2^2 - \alpha_{222}\mathcal{Q}_2^3.\end{aligned} \tag{C13}$$

The expansion coefficients read

$$\begin{aligned}\alpha_{111} &= \frac{\Delta_1^3}{6\pi\Delta^3} - \frac{\Delta_1}{2\pi\Delta},\quad \alpha_{112} = -\frac{\Delta_2^3}{2\pi\Delta^3},\\ \alpha_{122} &= -\frac{\Delta_1^3}{2\pi\Delta^3},\quad \alpha_{222} = \frac{\Delta_2^3}{6\pi\Delta^3} - \frac{\Delta_2}{2\pi\Delta}.\end{aligned} \tag{C14}$$

Rotation into the diagonal basis simplifies the cubic term considerably:

$$\mathcal{S}^{(3)} = -\frac{1}{3\pi}\mathcal{C}_1^3 - \frac{1}{2\pi}\mathcal{C}_1\mathcal{C}_2^2. \tag{C15}$$

Here, the second term gapes the spectrum of the field $\mathcal{C}_2$. Next we determine the fourth-order term

$$\tfrac{1}{4}\mathrm{tr}(G\vec{\mathcal{Q}}\cdot\hat{\Sigma})^4 = \beta_{1111}\mathcal{Q}_1^4 + \beta_{1112}\mathcal{Q}_1^3\mathcal{Q}_2 + (\beta_{1122}+\beta_{1212}) \times \mathcal{Q}_1^2\mathcal{Q}_2^2 + \beta_{1222}\mathcal{Q}_1\mathcal{Q}_2^3 + \beta_{2222}\mathcal{Q}_2^4, \quad \text{(C16)}$$

where

$$\beta_{1111} = \frac{\Delta_2^4}{8\pi\Delta^5}, \quad \beta_{1112} = -\frac{\Delta_1\Delta_2^3}{2\pi\Delta}, \quad \beta_{1122} = \frac{\Delta_1^4 + 4\Delta_1^2\Delta_2^2 + \Delta_2^4}{4\pi\Delta^5}, \quad \text{(C17)}$$

$$\beta_{1212} = -\frac{\Delta_1^4 + \Delta_1^2\Delta_2^2 + \Delta_2^4}{4\pi\Delta^5}, \quad \beta_{1222} = -\frac{\Delta_1^3\Delta_2}{2\pi\Delta}, \quad \beta_{2222} = \frac{\Delta_1^4}{8\pi\Delta^5}. \quad \text{(C18)}$$

Rotation into the diagonal basis simplifies strongly the structure of the fourth-order term:

$$\mathcal{S}^{(4)} = \frac{1}{8\pi\Delta}\mathcal{C}_2^4. \quad \text{(C19)}$$

The whole action to fourth order reads

$$\mathcal{S}[\mathcal{C}_1,\mathcal{C}_2] \approx \mathcal{C}_1\cdot E_H\mathcal{C}_1 - \frac{1}{3\pi}\mathcal{C}_1^3 + \mathcal{C}_2\cdot E_G\mathcal{C}_2 - \frac{1}{2\pi}\mathcal{C}_1\mathcal{C}_2^2 + \frac{1}{8\pi\Delta}\mathcal{C}_2^4. \quad \text{(C20)}$$

The effective potential reads ($\mathcal{S} = \int\mathcal{L} = \int[K-V]$, K staying for kinetic and V for potential energy)

$$V[\mathcal{C}_1,\mathcal{C}_2] \approx -\frac{\Delta}{2\pi}\mathcal{C}_1^2 + \frac{1}{3\pi}\mathcal{C}_1^3 + \frac{1}{2\pi}\mathcal{C}_1\mathcal{C}_2^2 - \frac{1}{8\pi\Delta}\mathcal{C}_2^4, \quad \text{(C21)}$$

which suggests a complex landscape. The minima of the potential follow from variations

$$\frac{\delta}{\delta\mathcal{C}_1}V[\mathcal{C}_1,\mathcal{C}_2] = 0 = -\frac{\Delta}{\pi}\mathcal{C}_1 + \frac{1}{\pi}\mathcal{C}_1^2 + \frac{1}{2\pi}\mathcal{C}_2^2, \quad \text{(C22)}$$

$$\frac{\delta}{\delta\mathcal{C}_2}V[\mathcal{C}_1,\mathcal{C}_2] = 0 = \frac{1}{\pi}\mathcal{C}_1\mathcal{C}_2 - \frac{1}{2\pi\Delta}\mathcal{C}_2^3. \quad \text{(C23)}$$

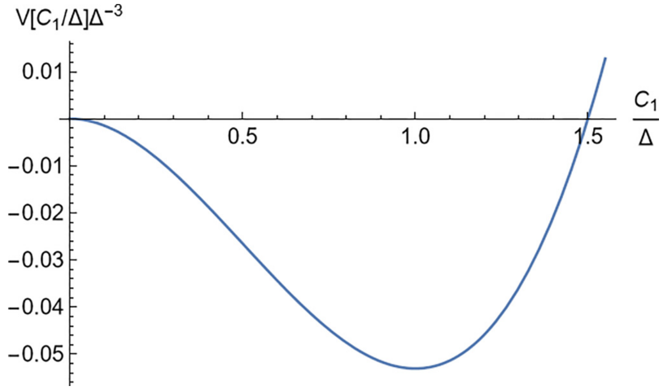

FIG. 3. The projection of the effective potential in Eq. (C21) on the line $\mathcal{C}_2 = 0$.

The trivial solution is $\mathcal{C}_1 = 0$, $\mathcal{C}_2 = 0$. Another possibility, which follows from the second equation is $\mathcal{C}_1 = \mathcal{C}_2^2/(2\Delta)$, which upon inserting into the first equation leads to $\mathcal{C}_2^4 = 0$. Finally, there is the third possibility, $\mathcal{C}_2 = 0$ and $\mathcal{C}_1 = \Delta$. The second derivative with respect to the fields taken at this extremum

$$\frac{\delta^2}{\delta\mathcal{C}_1^2}V[\mathcal{C}_1,\mathcal{C}_2]\bigg|_{\mathcal{C}_1=\Delta} = \frac{\Delta}{\pi}, \quad \text{(C24)}$$

is positive, and therefore the extremum is a local minimum on the $\mathcal{C}_1$ axis and a maximum on the $\mathcal{C}_2$ axis, i.e., it is a saddle point, which corresponds to a stable phase. The cut through the potential along the line $\mathcal{C}_2 = 0$ is shown in Fig. 3. At this point, the gapless fluctuations effectively decouple from the gaped

$$\mathcal{S}[\mathcal{C}_2] \approx \mathcal{C}_2\cdot\left[-\frac{\partial_\mu^2}{8\pi\Delta}\right]\mathcal{C}_2 - \frac{\Delta}{2\pi}\mathcal{C}_2^2 + \frac{1}{8\pi\Delta}\mathcal{C}_2^4, \quad \text{(C25)}$$

for the price of losing its gaplessness. This effect might be regarded as the Higgs mechanism, which forbids gapless fluctuations of the superconducting order parameter. Rescaling the variables $\mathcal{C}_2 \to \sqrt{2}\Delta\varphi$ we obtain the usual φ^4 model Eq. (24) with Ising symmetry.

[1] Y. E. Lozovik and V. I. Yudson, Pis'ma Zh. Eksp. Teor. Fiz. **22**, 556 (1975) [JETP Lett. **22**, 274 (1975)].

[2] Y. E. Lozovik and V. I. Yudson, Pis'ma Zh. Eksp. Teor. Fiz. **22**, 26 (1975) [JETP Lett. **22**, 11 (1975)].

[3] A. I. Liechtenstein, O. Gunnarsson, O. K. Andersen, and R. M. Martin, Phys. Rev. B **54**, 12505 (1996).

[4] M. Kellogg, I. B. Spielman, J. P. Eisenstein, L. N. Pfeiffer, and K. W. West, Phys. Rev. Lett. **88**, 126804 (2002).

[5] I. B. Spielman, M. Kellogg, J. P. Eisenstein, L. N. Pfeiffer, and K. W. West, Phys. Rev. B **70**, 081303 (2004).

[6] Y. E. Lozovik and A. A. Sokolik, JETP Lett. **87**, 55 (2008).

[7] M. P. Mink, H. T. C. Stoof, R. A. Duine, and A. H. MacDonald, Phys. Rev. B **84**, 155409 (2011).

[8] I. V. Blinov and A. H. MacDonald, Phys. Rev. B **106**, 224504 (2022).

[9] H. Min, R. Bistritzer, J.-J. Su, and A. H. MacDonald, Phys. Rev. B **78**, 121401 (2008).

[10] Y. Cao, V. Fatemi, S. Fang, K. Watanabe, T. Taniguchi, E. Kaxiras, and P. Jarillo-Herrero, Nature (London) **556**, 43 (2018).

[11] Y. Cao, V. Fatemi, A. Demir, S. Fang, S. L. Tomarken, J. Y. Luo, J. D. Sanchez-Yamagishi, K. Watanabe, T. Taniguchi, E. Kaxiras *et al.*, Nature (London) **556**, 80 (2018).

[12] R. Bistritzer and A. H. MacDonald, Proc. Natl. Acad. Sci. USA **108**, 12233 (2011).

[13] J. M. B. Lopes dos Santos, N. M. R. Peres, and A. H. Castro Neto, Phys. Rev. Lett. **99**, 256802 (2007).

[14] J. P. Eisenstein and A. H. MacDonald, Nature (London) **432**, 691 (2004).

[15] A. Sinner, Y. E. Lozovik, and K. Ziegler, Phys. Rev. Res. **2**, 033085 (2020).

[16] A. Sinner, Y. E. Lozovik, and K. Ziegler, Phys. Rev. B **104**, 245124 (2021).
[17] K. Ziegler, A. Sinner, and Y. E. Lozovik, Phys. Rev. Lett. **128**, 157001 (2022).
[18] J. I. A. Li, T. Taniguchi, K. Watanabe, J. Hone, and C. R. Dean, Nat. Phys. **13**, 751 (2017).
[19] X. Liu, Z. Hao, K. Watanabe, T. Taniguchi, B. I. Halperin, and P. Kim, Nat. Phys. **15**, 893 (2019).
[20] J. I. A. Li, Q. Shi, Y. Zeng, K. Watanabe, T. Taniguchi, J. Hone, and C. R. Dean, Nat. Phys. **15**, 898 (2019).
[21] J. K. Jain, Phys. Rev. Lett. **63**, 199 (1989).
[22] S. C. Zhang, T. H. Hansson, and S. Kivelson, Phys. Rev. Lett. **62**, 82 (1989).
[23] D.-H. Lee and S.-C. Zhang, Phys. Rev. Lett. **66**, 1220 (1991).
[24] Y.-P. Lin and R. M. Nandkishore, Phys. Rev. B **100**, 085136 (2019).
[25] R. Nandkishore, L. S. Levitov, and A. V. Chubukov, Nat. Phys. **8**, 158 (2012).
[26] I. F. Herbut, V. Juričić, and O. Vafek, Phys. Rev. B **80**, 075432 (2009).
[27] O. Vafek and K. Yang, Phys. Rev. B **81**, 041401 (2010).
[28] O. Vafek, Phys. Rev. B **82**, 205106 (2010).
[29] S. Uebelacker and C. Honerkamp, Phys. Rev. B **84**, 205122 (2011).
[30] M. M. Scherer, S. Uebelacker, and C. Honerkamp, Phys. Rev. B **85**, 235408 (2012).
[31] Y. Xu, X. Li, and J. Dong, Nanotechnology **21**, 065711 (2010).
[32] M. Fierz, Z. Phys. **104**, 553 (1937).
[33] A. Sinner and K. Ziegler, Ann. Phys. **400**, 262 (2019).
[34] E. J. Weinberg, Annu. Rev. Nucl. Part. Sci. **42**, 177 (1992).
[35] A. Lopez and E. Fradkin, Phys. Rev. B **44**, 5246 (1991).
[36] S. C. Zhang, Int. J. Mod. Phys. B **06**, 25 (1992).
[37] Y.-M. Lu and A. Vishwanath, Phys. Rev. B **86**, 125119 (2012).
[38] G. V. Dunne, *Topological Aspects of Low Dimensional Systems, Les Houches Summer School*, edited by A. Comtet, T. Jolicoeur, S. Ouvry, and F. David (Springer, Berlin, 1999), Vol. 69, pp. 177–263.
[39] S. Deser, R. Jackiw, and S. Templeton, Phys. Rev. Lett. **48**, 975 (1982).
[40] H. J. de Vega and F. A. Schaposnik, Phys. Rev. Lett. **56**, 2564 (1986).
[41] E. Fradkin, *Field Theories of Condensed Matter Physics*, 2nd ed. (Cambridge University Press, Cambridge, 2013).
[42] D. Tong, Lectures on the quantum Hall effect, http://www.damtp.cam.ac.uk/user/tong/qhe.html.
[43] A. Stern, Ann. Phys. **323**, 204 (2008).
[44] H. L. Stormer, Rev. Mod. Phys. **71**, 875 (1999).